Chapter 16

$\mathcal{H}_\infty$ Loop Shaping

This chapter introduces a design technique that incorporates loop-shaping methods to obtain performance/robust stability tradeoffs, and a particular $\mathcal{H}_\infty$ optimization problem to guarantee closed-loop stability and a level of robust stability at all frequencies. The proposed technique uses only the basic concept of loop-shaping methods, and then a robust stabilization controller for the normalized coprime factor perturbed system is used to construct the final controller. This chapter is arranged as follows: The $\mathcal{H}_\infty$ theory is applied to solve the stabilization problem of a normalized coprime factor perturbed system in Section 16.1. The loop-shaping design procedure is described in Section 16.2. The theoretical justification for the loop-shaping design procedure is given in Section 16.3. Some further loop-shaping guidelines are given in Section 16.4.

16.1 Robust Stabilization of Coprime Factors

In this section, we use the $\mathcal{H}_\infty$ control theory developed in previous chapters to solve the robust stabilization of a left coprime factor perturbed plant given by

$$P_\Delta = (\tilde{M} + \tilde{\Delta}_M)^{-1}(\tilde{N} + \tilde{\Delta}_N)$$

with $\tilde{M}, \tilde{N}, \tilde{\Delta}_M, \tilde{\Delta}_N \in \mathcal{RH}_\infty$ and $\left\| \begin{bmatrix} \tilde{\Delta}_N & \tilde{\Delta}_M \end{bmatrix} \right\|_\infty < \epsilon$ (see Figure 16.1). The transfer matrices $(\tilde{M}, \tilde{N})$ are assumed to be a left coprime factorization of P (i.e., $P = \tilde{M}^{-1}\tilde{N}$), and K internally stabilizes the nominal system.

It has been shown in Chapter 8 that the system is robustly stable iff

$$\left\| \begin{bmatrix} K \\ I \end{bmatrix} (I + PK)^{-1}\tilde{M}^{-1} \right\|_\infty \leq 1/\epsilon.$$

Finding a controller such that the above norm condition holds is an $\mathcal{H}_\infty$ norm minimization problem that can be solved using $\mathcal{H}_\infty$ theory developed in previous chapters.

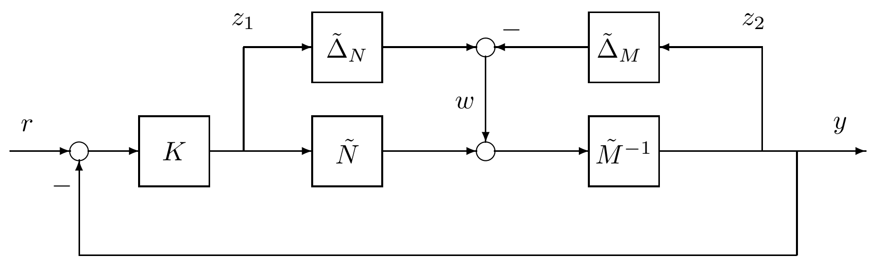

Figure 16.1: Left coprime factor perturbed systems

Suppose P has a stabilizable and detectable state-space realization given by

$$P = \left[\begin{array}{c|c} A & B \\ \hline C & D \end{array}\right]$$

and let L be a matrix such that $A + LC$ is stable. Then a left coprime factorization of $P = \tilde{M}^{-1}\tilde{N}$ is given by

$$\left[\begin{array}{cc} \tilde{N} & \tilde{M} \end{array}\right] = \left[\begin{array}{c|cc} A + LC & B + LD & L \\ \hline ZC & ZD & Z \end{array}\right]$$

where Z can be any nonsingular matrix. In particular, we shall choose $Z = (I + DD^*)^{-1/2}$ if $P = \tilde{M}^{-1}\tilde{N}$ is chosen to be a normalized left coprime factorization. Denote

$$\hat{K} = -K.$$

Then the system diagram can be put in an LFT form, as in Figure 16.2, with the generalized plant

$$G(s) = \left[\begin{array}{cc} \left[\begin{array}{c} 0 \\ \tilde{M}^{-1} \end{array}\right] & \left[\begin{array}{c} I \\ P \end{array}\right] \\ \tilde{M}^{-1} & P \end{array}\right] = \left[\begin{array}{c|cc} A & -LZ^{-1} & B \\ \hline \left[\begin{array}{c} 0 \\ C \end{array}\right] & \left[\begin{array}{c} 0 \\ Z^{-1} \end{array}\right] & \left[\begin{array}{c} I \\ D \end{array}\right] \\ C & Z^{-1} & D \end{array}\right]$$

$$=: \left[\begin{array}{c|cc} A & B_1 & B_2 \\ \hline C_1 & D_{11} & D_{12} \\ C_2 & D_{21} & D_{22} \end{array}\right].$$

To apply the $\mathcal{H}_\infty$ control formulas in Chapter 14, we need to normalize the D_{12} and D_{21} first. Note that

$$\left[\begin{array}{c} I \\ D \end{array}\right] = U \left[\begin{array}{c} 0 \\ I \end{array}\right] (I + D^*D)^{\frac{1}{2}}, \quad \text{where } U = \left[\begin{array}{cc} D^*(I + DD^*)^{-\frac{1}{2}} & (I + D^*D)^{-\frac{1}{2}} \\ -(I + DD^*)^{-\frac{1}{2}} & D(I + D^*D)^{-\frac{1}{2}} \end{array}\right]$$

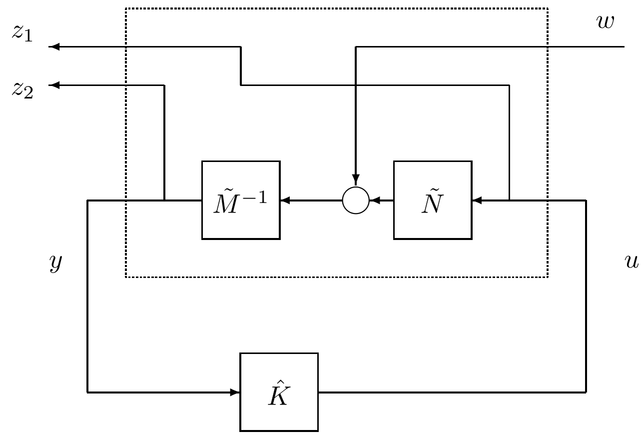

Figure 16.2: LFT diagram for coprime factor stabilization

and U is a unitary matrix. Let

$$\begin{aligned} \hat{K} &= (I + D^*D)^{-\frac{1}{2}}\tilde{K}Z \\ \begin{bmatrix} z_1 \\ z_2 \end{bmatrix} &= U \begin{bmatrix} \hat{z}_1 \\ \hat{z}_2 \end{bmatrix}. \end{aligned}$$

Then $\|T_{zw}\|_\infty = \|U^*T_{zw}\|_\infty = \|T_{\hat{z}w}\|_\infty$ and the problem becomes one of finding a controller $\tilde{K}$ so that $\|T_{\hat{z}w}\|_\infty < \gamma$ with the following generalized plant:

$$\hat{G} = \begin{bmatrix} U^* & 0 \\ 0 & Z \end{bmatrix} G \begin{bmatrix} I & 0 \\ 0 & (I + D^*D)^{-\frac{1}{2}} \end{bmatrix}$$

$$= \left[\begin{array}{c|cc} A & -LZ^{-1} & B \\ \hline \begin{bmatrix} -(I + DD^*)^{-\frac{1}{2}}C \\ (I + D^*D)^{-\frac{1}{2}}D^*C \end{bmatrix} & \begin{bmatrix} -(I + DD^*)^{-\frac{1}{2}}Z^{-1} \\ (I + D^*D)^{-\frac{1}{2}}D^*Z^{-1} \end{bmatrix} & \begin{bmatrix} 0 \\ I \end{bmatrix} \\ ZC & I & ZD(I + D^*D)^{-\frac{1}{2}} \end{array}\right].$$

Now the formulas in Chapter 14 can be applied to $\hat{G}$ to obtain a controller $\tilde{K}$ and then the K can be obtained from $K = -(I + D^*D)^{-\frac{1}{2}}\tilde{K}Z$. We shall leave the detail to the reader. In the sequel, we shall consider the case $D = 0$ and $Z = I$. In this case, we have $\gamma > 1$ and

$$X_\infty(A - \frac{LC}{\gamma^2 - 1}) + (A - \frac{LC}{\gamma^2 - 1})^*X_\infty - X_\infty(BB^* - \frac{LL^*}{\gamma^2 - 1})X_\infty + \frac{\gamma^2C^*C}{\gamma^2 - 1} = 0$$

$$Y_\infty(A + LC)^* + (A + LC)Y_\infty - Y_\infty C^*CY_\infty = 0.$$

It is clear that $Y_\infty = 0$ is the stabilizing solution. Hence by the formulas in Chapter 14 we have

$$\begin{bmatrix} L_{1\infty} & L_{2\infty} \end{bmatrix} = \begin{bmatrix} 0 & L \end{bmatrix}$$

and

$$Z_\infty = I, \quad \hat{D}_{11} = 0, \quad \hat{D}_{12} = I, \quad \hat{D}_{21} = \frac{\sqrt{\gamma^2 - 1}}{\gamma} I.$$

The results are summarized in the following theorem.

Theorem 16.1 *Let $D = 0$ and let L be such that $A + LC$ is stable. Then there exists a controller K such that*

$$\left\| \begin{bmatrix} K \\ I \end{bmatrix} (I + PK)^{-1} \tilde{M}^{-1} \right\|_\infty < \gamma$$

iff $\gamma > 1$ and there exists a stabilizing solution $X_\infty \geq 0$ solving

$$X_\infty (A - \frac{LC}{\gamma^2 - 1}) + (A - \frac{LC}{\gamma^2 - 1})^* X_\infty - X_\infty (BB^* - \frac{LL^*}{\gamma^2 - 1}) X_\infty + \frac{\gamma^2 C^* C}{\gamma^2 - 1} = 0.$$

Moreover, if the above conditions hold a central controller is given by

$$K = \left[\begin{array}{c|c} A - BB^* X_\infty + LC & L \\ \hline - B^* X_\infty & 0 \end{array} \right].$$

It is clear that the existence of a robust stabilizing controller depends on the choice of the stabilizing matrix L (i.e., the choice of the coprime factorization). Now let $Y \geq 0$ be the stabilizing solution to

$$AY + YA^* - YC^*CY + BB^* = 0$$

and let $L = -YC^*$. Then the left coprime factorization $(\tilde{M}, \tilde{N})$ given by

$$\begin{bmatrix} \tilde{N} & \tilde{M} \end{bmatrix} = \left[\begin{array}{c|cc} A - YC^*C & B & -YC^* \\ \hline C & 0 & I \end{array} \right]$$

is a normalized left coprime factorization (see Chapter 12). Let $\|\cdot\|_H$ denote the Hankel norm (i.e., the largest Hankel singular value). Then we have the following result.

Corollary 16.2 *Let $D = 0$ and $L = -YC^*$, where $Y \geq 0$ is the stabilizing solution to*

$$AY + YA^* - YC^*CY + BB^* = 0.$$

Then $P = \tilde{M}^{-1}\tilde{N}$ is a normalized left coprime factorization and

$$\begin{aligned} \inf_{K \text{ stabilizing}} \left\| \begin{bmatrix} K \\ I \end{bmatrix} (I + PK)^{-1} \tilde{M}^{-1} \right\|_\infty &= \frac{1}{\sqrt{1 - \lambda_{\max}(YQ)}} \\ &= \left(1 - \left\| \begin{bmatrix} \tilde{N} & \tilde{M} \end{bmatrix} \right\|_H^2 \right)^{-1/2} =: \gamma_{\min} \end{aligned}$$

where Q is the solution to the following Lyapunov equation:

$$Q(A - YC^*C) + (A - YC^*C)^*Q + C^*C = 0.$$

Moreover, if the preceding conditions hold, then for any $\gamma > \gamma_{\min}$ a controller achieving

$$\left\| \begin{bmatrix} K \\ I \end{bmatrix} (I + PK)^{-1}\tilde{M}^{-1} \right\|_\infty < \gamma$$

is given by

$$K(s) = \left[\begin{array}{c|c} A - BB^*X_\infty - YC^*C & -YC^* \\ \hline -B^*X_\infty & 0 \end{array} \right]$$

where

$$X_\infty = \frac{\gamma^2}{\gamma^2 - 1} Q \left(I - \frac{\gamma^2}{\gamma^2 - 1} YQ \right)^{-1}.$$

Proof. Note that the Hamiltonian matrix associated with X_∞ is given by

$$H_\infty = \begin{bmatrix} A + \frac{1}{\gamma^2-1} YC^*C & -BB^* + \frac{1}{\gamma^2-1} YC^*CY \\ -\frac{\gamma^2}{\gamma^2-1} C^*C & -(A + \frac{1}{\gamma^2-1} YC^*C)^* \end{bmatrix}.$$

Straightforward calculation shows that

$$H_\infty = \begin{bmatrix} I & -\frac{\gamma^2}{\gamma^2-1} Y \\ 0 & \frac{\gamma^2}{\gamma^2-1} I \end{bmatrix} H_q \begin{bmatrix} I & -\frac{\gamma^2}{\gamma^2-1} Y \\ 0 & \frac{\gamma^2}{\gamma^2-1} I \end{bmatrix}^{-1}$$

where

$$H_q = \begin{bmatrix} A - YC^*C & 0 \\ -C^*C & -(A - YC^*C)^* \end{bmatrix}.$$

It is clear that the stable invariant subspace of H_q is given by

$$\mathcal{X}_-(H_q) = \operatorname{Im} \begin{bmatrix} I \\ Q \end{bmatrix}$$

and the stable invariant subspace of H_∞ is given by

$$\mathcal{X}_-(H_\infty) = \begin{bmatrix} I & -\frac{\gamma^2}{\gamma^2-1} Y \\ 0 & \frac{\gamma^2}{\gamma^2-1} I \end{bmatrix} \mathcal{X}_-(H_q) = \operatorname{Im} \begin{bmatrix} I - \frac{\gamma^2}{\gamma^2-1} YQ \\ \frac{\gamma^2}{\gamma^2-1} Q \end{bmatrix}.$$

Hence there is a nonnegative definite stabilizing solution to the algebraic Riccati equation of X_∞ if and only if

$$I - \frac{\gamma^2}{\gamma^2 - 1} YQ > 0$$

or

$$\gamma > \frac{1}{\sqrt{1-\lambda_{\max}(YQ)}}$$

and the solution, if it exists, is given by

$$X_\infty = \frac{\gamma^2}{\gamma^2-1} Q \left(I - \frac{\gamma^2}{\gamma^2-1} YQ\right)^{-1}.$$

Note that Y and Q are the controllability Gramian and the observability Gramian of $\begin{bmatrix} \tilde{N} & \tilde{M} \end{bmatrix}$ respectively. Therefore, we also have that the Hankel norm of $\begin{bmatrix} \tilde{N} & \tilde{M} \end{bmatrix}$ is $\sqrt{\lambda_{\max}(YQ)}$. $\square$

Corollary 16.3 *Let $P = \tilde{M}^{-1}\tilde{N}$ be a normalized left coprime factorization and*

$$P_\Delta = (\tilde{M} + \tilde{\Delta}_M)^{-1}(\tilde{N} + \tilde{\Delta}_N)$$

with

$$\left\| \begin{bmatrix} \tilde{\Delta}_N & \tilde{\Delta}_M \end{bmatrix} \right\|_\infty < \epsilon.$$

Then there is a robustly stabilizing controller for P_Δ if and only if

$$\epsilon \le \sqrt{1-\lambda_{\max}(YQ)} = \sqrt{1 - \left\| \begin{bmatrix} \tilde{N} & \tilde{M} \end{bmatrix} \right\|_H^2}.$$

The solutions to the normalized left coprime factorization stabilization problem are also solutions to a related $\mathcal{H}_\infty$ problem, which is shown in the following lemma.

Lemma 16.4 *Let $P = \tilde{M}^{-1}\tilde{N}$ be a normalized left coprime factorization. Then*

$$\left\| \begin{bmatrix} K \\ I \end{bmatrix} (I+PK)^{-1}\tilde{M}^{-1} \right\|_\infty = \left\| \begin{bmatrix} K \\ I \end{bmatrix} (I+PK)^{-1} \begin{bmatrix} I & P \end{bmatrix} \right\|_\infty.$$

Proof. Since $(\tilde{M}, \tilde{N})$ is a normalized left coprime factorization of P, we have

$$\begin{bmatrix} \tilde{M} & \tilde{N} \end{bmatrix} \begin{bmatrix} \tilde{M} & \tilde{N} \end{bmatrix}^\sim = I$$

and

$$\left\| \begin{bmatrix} \tilde{M} & \tilde{N} \end{bmatrix} \right\|_\infty = \left\| \begin{bmatrix} \tilde{M} & \tilde{N} \end{bmatrix}^\sim \right\|_\infty = 1.$$

Using these equations, we have

$$\left\| \begin{bmatrix} K \\ I \end{bmatrix} (I+PK)^{-1}\tilde{M}^{-1} \right\|_\infty$$

$$
\begin{aligned}
&= \left\| \begin{bmatrix} K \\ I \end{bmatrix} (I+PK)^{-1}\tilde{M}^{-1} \begin{bmatrix} \tilde{M} & \tilde{N} \end{bmatrix} \begin{bmatrix} \tilde{M} & \tilde{N} \end{bmatrix}^{\sim} \right\|_{\infty} \\
&\leq \left\| \begin{bmatrix} K \\ I \end{bmatrix} (I+PK)^{-1}\tilde{M}^{-1} \begin{bmatrix} \tilde{M} & \tilde{N} \end{bmatrix} \right\|_{\infty} \left\| \begin{bmatrix} \tilde{M} & \tilde{N} \end{bmatrix}^{\sim} \right\|_{\infty} \\
&= \left\| \begin{bmatrix} K \\ I \end{bmatrix} (I+PK)^{-1} \begin{bmatrix} I & P \end{bmatrix} \right\|_{\infty} \\
&\leq \left\| \begin{bmatrix} K \\ I \end{bmatrix} (I+PK)^{-1}\tilde{M}^{-1} \right\|_{\infty} \left\| \begin{bmatrix} \tilde{M} & \tilde{N} \end{bmatrix} \right\|_{\infty} \\
&= \left\| \begin{bmatrix} K \\ I \end{bmatrix} (I+PK)^{-1}\tilde{M}^{-1} \right\|_{\infty}.
\end{aligned}
$$

This implies

$$
\left\| \begin{bmatrix} K \\ I \end{bmatrix} (I+PK)^{-1}\tilde{M}^{-1} \right\|_{\infty} = \left\| \begin{bmatrix} K \\ I \end{bmatrix} (I+PK)^{-1} \begin{bmatrix} I & P \end{bmatrix} \right\|_{\infty}.
$$

□

Combining Corollary 16.3 and Lemma 16.4, we have the following result.

Corollary 16.5 *A controller solves the normalized left coprime factor robust stabilization problem if and only if it solves the following $\mathcal{H}_\infty$ control problem:*

$$
\left\| \begin{bmatrix} I \\ K \end{bmatrix} (I+PK)^{-1} \begin{bmatrix} I & P \end{bmatrix} \right\|_{\infty} < \gamma
$$

and

$$
\begin{aligned}
\inf_{K \text{ stabilizing}} \left\| \begin{bmatrix} I \\ K \end{bmatrix} (I+PK)^{-1} \begin{bmatrix} I & P \end{bmatrix} \right\|_{\infty} &= \frac{1}{\sqrt{1-\lambda_{\max}(YQ)}} \\
&= \left(1 - \left\| \begin{bmatrix} \tilde{N} & \tilde{M} \end{bmatrix} \right\|_H^2 \right)^{-1/2}.
\end{aligned}
$$

The solution Q can also be obtained in other ways. Let $X \geq 0$ be the stabilizing solution to

$$
XA + A^*X - XBB^*X + C^*C = 0.
$$

Then it is easy to verify that

$$
Q = (I+XY)^{-1}X.
$$

Hence

$$\gamma_{\min} = \frac{1}{\sqrt{1-\lambda_{\max}(YQ)}} = \left(1 - \left\| \begin{bmatrix} \tilde{N} & \tilde{M} \end{bmatrix} \right\|_H^2 \right)^{-1/2} = \sqrt{1+\lambda_{\max}(XY)}.$$

Similar results can be obtained if one starts with a normalized right coprime factorization. In fact, a rather strong relation between the normalized left and right coprime factorization problems can be established using the following matrix fact.

Lemma 16.6 *Let M be a square matrix such that $M^2 = M$. Then $\sigma_i(M) = \sigma_i(I-M)$ for all i such that $0 < \sigma_i(M) \neq 1$.*

Proof. We first show that the eigenvalues of M are either 0 or 1 and M is diagonalizable. In fact, assume that λ is an eigenvalue of M and x is a corresponding eigenvector. Then $\lambda x = Mx = MMx = M(Mx) = \lambda Mx = \lambda^2 x$; that is, $\lambda(1-\lambda)x = 0$. This implies that either $\lambda = 0$ or $\lambda = 1$. To show that M is diagonalizable, assume that $M = TJT^{-1}$, where J is a Jordan canonical form. It follows immediately that J must be diagonal by the condition $M = M^2$.

Next, assume that M is diagonalized by a nonsingular matrix T such that

$$M = T \begin{bmatrix} I & 0 \\ 0 & 0 \end{bmatrix} T^{-1}.$$

Then

$$N := I - M = T \begin{bmatrix} 0 & 0 \\ 0 & I \end{bmatrix} T^{-1}.$$

Define

$$\begin{bmatrix} A & B \\ B^* & D \end{bmatrix} := T^*T$$

and assume $0 < \lambda \neq 1$. Then $A > 0$ and

$$\begin{aligned}
& \det(M^*M - \lambda I) = 0 \\
\Leftrightarrow \quad & \det(\begin{bmatrix} I & 0 \\ 0 & 0 \end{bmatrix} T^*T \begin{bmatrix} I & 0 \\ 0 & 0 \end{bmatrix} - \lambda T^*T) = 0 \\
\Leftrightarrow \quad & \det \begin{bmatrix} (1-\lambda)A & -\lambda B \\ -\lambda B^* & -\lambda D \end{bmatrix} = 0 \\
\Leftrightarrow \quad & \det(-\lambda D - \frac{\lambda^2}{1-\lambda} B^* A^{-1} B) = 0 \\
\Leftrightarrow \quad & \det(\frac{1-\lambda}{\lambda} D + B^* A^{-1} B) = 0
\end{aligned}$$

$$\begin{aligned}
&\Leftrightarrow \quad \det \begin{bmatrix} -\lambda A & -\lambda B \\ -\lambda B^* & (1-\lambda)D \end{bmatrix} = 0 \\
&\Leftrightarrow \quad \det(N^*N - \lambda I) = 0.
\end{aligned}$$

This implies that all nonzero eigenvalues of M^*M and N^*N that are not equal to 1 are equal; that is, $\sigma_i(M) = \sigma_i(I - M)$ for all i such that $0 < \sigma_i(M) \neq 1$. □

Using this matrix fact, we have the following corollary.

Corollary 16.7 *Let K and P be any compatibly dimensioned complex matrices. Then*

$$\left\| \begin{bmatrix} I \\ K \end{bmatrix} (I + PK)^{-1} \begin{bmatrix} I & P \end{bmatrix} \right\| = \left\| \begin{bmatrix} I \\ P \end{bmatrix} (I + KP)^{-1} \begin{bmatrix} I & K \end{bmatrix} \right\|.$$

Proof. Define

$$M = \begin{bmatrix} I \\ K \end{bmatrix} (I + PK)^{-1} \begin{bmatrix} I & P \end{bmatrix}, \quad N = \begin{bmatrix} -P \\ I \end{bmatrix} (I + KP)^{-1} \begin{bmatrix} -K & I \end{bmatrix}.$$

Then it is easy to verify that $M^2 = M$ and $N = I - M$. By Lemma 16.6, we have $\|M\| = \|N\|$. The corollary follows by noting that

$$\begin{bmatrix} I \\ P \end{bmatrix} (I + KP)^{-1} \begin{bmatrix} I & K \end{bmatrix} = \begin{bmatrix} 0 & I \\ -I & 0 \end{bmatrix} N \begin{bmatrix} 0 & -I \\ I & 0 \end{bmatrix}.$$

□

Corollary 16.8 *Let $P = \tilde{M}^{-1}\tilde{N} = NM^{-1}$ be, respectively, the normalized left and right coprime factorizations. Then*

$$\left\| \begin{bmatrix} K \\ I \end{bmatrix} (I + PK)^{-1} \tilde{M}^{-1} \right\|_\infty = \left\| M^{-1}(I + KP)^{-1} \begin{bmatrix} I & K \end{bmatrix} \right\|_\infty.$$

Proof. This follows from Corollary 16.7 and the fact that

$$\left\| M^{-1}(I + KP)^{-1} \begin{bmatrix} I & K \end{bmatrix} \right\|_\infty = \left\| \begin{bmatrix} I \\ P \end{bmatrix} (I + KP)^{-1} \begin{bmatrix} I & K \end{bmatrix} \right\|_\infty.$$

□

This corollary says that any $\mathcal{H}_\infty$ controller for the normalized left coprime factorization is also an $\mathcal{H}_\infty$ controller for the normalized right coprime factorization. Hence one can work with either factorization.

For future reference, we shall define

$$b_{P,K} := \begin{cases} \left(\left\| \begin{bmatrix} I \\ K \end{bmatrix} (I+PK)^{-1} \begin{bmatrix} I & P \end{bmatrix} \right\|_\infty \right)^{-1} & \text{if } K \text{ stabilizes } P \\ \\ 0 & \text{otherwise} \end{cases}$$

and

$$b_{\rm opt} := \sup_K b_{P,K}.$$

Then $b_{P,K} = b_{K,P}$ and

$$b_{\rm opt} = \sqrt{1 - \lambda_{\max}(YQ)} = \sqrt{1 - \left\| \begin{bmatrix} \tilde{N} & \tilde{M} \end{bmatrix} \right\|_H^2}.$$

The number $b_{P,K}$ can be related to the classical gain and phase margins as shown in Vinnicombe [1993b].

Theorem 16.9 *Let P be a SISO plant and K be a stabilizing controller. Then*

$$\text{gain margin} \geq \frac{1 + b_{P,K}}{1 - b_{P,K}}$$

and

$$\text{phase margin} \geq 2 \arcsin(b_{P,K}).$$

Proof. Note that for SISO system

$$b_{P,K} \leq \frac{|1 + P(j\omega)K(j\omega)|}{\sqrt{1 + |P(j\omega)|^2}\sqrt{1 + |K(j\omega)|^2}}, \quad \forall \omega.$$

So, at frequencies where $k := -P(j\omega)K(j\omega) \in \mathbb{R}^+$,

$$b_{P,K} \leq \frac{|1-k|}{\sqrt{(1+|P|^2)(1+\frac{k^2}{|P|^2})}} \leq \frac{|1-k|}{\sqrt{\min_P \left\{ (1+|P|^2)(1+\frac{k^2}{|P|^2}) \right\}}} = \left| \frac{1-k}{1+k} \right|,$$

which implies that

$$k \leq \frac{1 - b_{P,K}}{1 + b_{P,K}}, \quad \text{or} \quad k \geq \frac{1 + b_{P,K}}{1 - b_{P,K}}$$

from which the gain margin result follows. Similarly, at frequencies where $P(j\omega)K(j\omega) = -e^{j\theta}$,

$$b_{P,K} \leq \frac{|1 - e^{j\theta}|}{\sqrt{(1+|P|^2)(1+\frac{1}{|P|^2})}} \leq \frac{|2\sin\frac{\theta}{2}|}{\sqrt{\min_P \left\{ (1+|P|^2)(1+\frac{1}{|P|^2}) \right\}}} = \frac{|2\sin\frac{\theta}{2}|}{2},$$

which implies $\theta \geq 2 \arcsin b_{P,K}$. □

For example, $b_{P,K} = 1/2$ guarantees a gain margin of 3 and a phase margin of 60°.

Illustrative MATLAB Commands:

$\gg$ $\mathbf{b_{p,k}} = \mathbf{emargin}(\mathbf{P}, \mathbf{K})$; % given P and K, compute $b_{P,K}$.

$\gg$ $[\mathbf{K}_{\text{opt}}, \mathbf{b_{p,k}}] = \mathbf{ncfsyn}(\mathbf{P}, \mathbf{1})$; % find the optimal controller K_{opt}.

$\gg$ $[\mathbf{K}_{\text{sub}}, \mathbf{b_{p,k}}] = \mathbf{ncfsyn}(\mathbf{P}, \mathbf{2})$; % find a suboptimal controller K_{sub}.

16.2 Loop-Shaping Design

This section considers the $\mathcal{H}_\infty$ loop-shaping design. The objective of this approach is to incorporate the simple performance/robustness tradeoff obtained in the loop-shaping with the guaranteed stability properties of $\mathcal{H}_\infty$ design methods. Recall from Section 6.1 of Chapter 6 that good performance controller design requires that

$$\overline{\sigma}\left((I+PK)^{-1}\right), \quad \overline{\sigma}\left((I+PK)^{-1}P\right), \quad \overline{\sigma}\left((I+KP)^{-1}\right), \quad \overline{\sigma}\left(K(I+PK)^{-1}\right) \tag{16.1}$$

be made small, particularly in some low-frequency range. Good robustness requires that

$$\overline{\sigma}\left(PK(I+PK)^{-1}\right), \quad \overline{\sigma}\left(KP(I+KP)^{-1}\right) \tag{16.2}$$

be made small, particularly in some high-frequency range. These requirements, in turn, imply that good controller design boils down to achieving the desired loop (and controller) gains in the appropriate frequency range:

$$\underline{\sigma}(PK) \gg 1, \quad \underline{\sigma}(KP) \gg 1, \quad \underline{\sigma}(K) \gg 1$$

in some low-frequency range and

$$\overline{\sigma}(PK) \ll 1, \quad \overline{\sigma}(KP) \ll 1, \quad \overline{\sigma}(K) \leq M$$

in some high-frequency range where M is not too large.

The $\mathcal{H}_\infty$ loop-shaping design procedure is developed by McFarlane and Glover [1990, 1992] and is stated next.

Loop-Shaping Design Procedure

(1) Loop-Shaping: The singular values of the nominal plant, as shown in Figure 16.3, are shaped, using a precompensator W_1 and/or a postcompensator W_2, to give a desired open-loop shape. The nominal plant P and the shaping functions W_1, W_2 are combined to form the shaped plant, P_s, where $P_s = W_2 P W_1$. We assume that W_1 and W_2 are such that P_s contains no hidden modes.

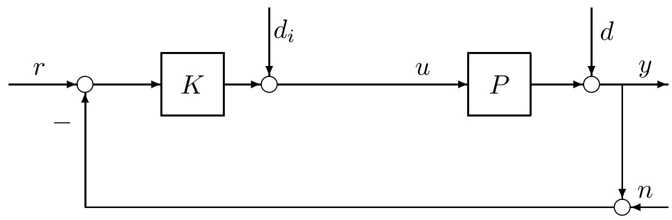

Figure 16.3: Standard feedback configuration

(2) Robust Stabilization: a) Calculate $\epsilon_{\max}$ (i.e., $b_{\text{opt}}(P_s)$), where

$$\begin{aligned}\epsilon_{\max} &= \left(\inf_{K \text{ stabilizing}} \left\| \begin{bmatrix} I \\ K \end{bmatrix} (I + P_s K)^{-1} \tilde{M}_s^{-1} \right\|_\infty \right)^{-1} \\ &= \sqrt{1 - \left\| \begin{bmatrix} \tilde{N}_s & \tilde{M}_s \end{bmatrix} \right\|_H^2} < 1\end{aligned}$$

and $\tilde{M}_s, \tilde{N}_s$ define the normalized coprime factors of P_s such that $P_s = \tilde{M}_s^{-1}\tilde{N}_s$ and

$$\tilde{M}_s \tilde{M}_s^\sim + \tilde{N}_s \tilde{N}_s^\sim = I.$$

If $\epsilon_{\max} \ll 1$ return to (1) and adjust W_1 and W_2.

b) Select $\epsilon \leq \epsilon_{\max}$; then synthesize a stabilizing controller K_∞ that satisfies

$$\left\| \begin{bmatrix} I \\ K_\infty \end{bmatrix} (I + P_s K_\infty)^{-1} \tilde{M}_s^{-1} \right\|_\infty \leq \epsilon^{-1}.$$

(3) The final feedback controller K is then constructed by combining the $\mathcal{H}_\infty$ controller K_∞ with the shaping functions W_1 and W_2, as shown in Figure 16.4, such that

$$K = W_1 K_\infty W_2.$$

A typical design works as follows: the designer inspects the open-loop singular values of the nominal plant and shapes these by pre- and/or postcompensation until nominal performance (and possibly robust stability) specifications are met. (Recall that the open-loop shape is related to closed-loop objectives.) A feedback controller K_∞ with associated stability margin (for the shaped plant) $\epsilon \leq \epsilon_{\max}$, is then synthesized. If $\epsilon_{\max}$ is small, then the specified loop shape is incompatible with robust stability requirements and should be adjusted accordingly; then K_∞ is reevaluated.

In the preceding design procedure we have specified the desired loop shape by $W_2 P W_1$. But after Stage (2) of the design procedure, the actual loop shape achieved

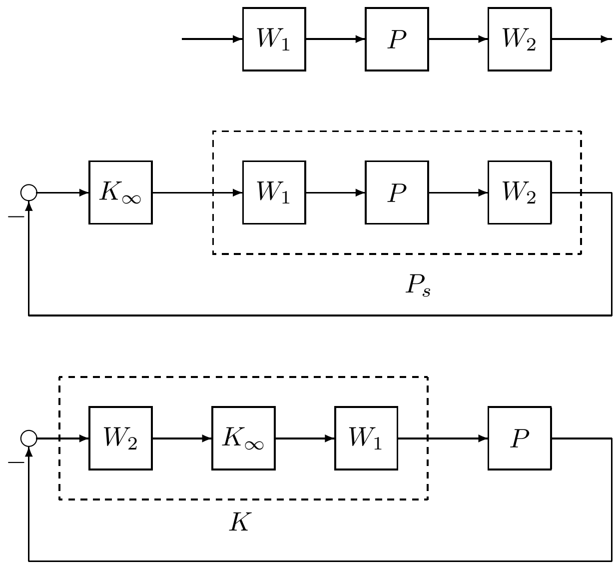

Figure 16.4: The loop-shaping design procedure

is, in fact, given by $W_1 K_\infty W_2 P$ at plant input and $P W_1 K_\infty W_2$ at plant output. It is therefore possible that the inclusion of K_∞ in the open-loop transfer function will cause deterioration in the open-loop shape specified by P_s. In the next section, we will show that the degradation in the loop shape caused by the $\mathcal{H}_\infty$ controller K_∞ is limited at frequencies where the specified loop shape is sufficiently large or sufficiently small. In particular, we show in the next section that ϵ can be interpreted as an indicator of the success of the loop-shaping in addition to providing a robust stability guarantee for the closed-loop systems. A small value of $\epsilon_{\max}$ ($\epsilon_{\max} \ll 1$) in Stage (2) always indicates incompatibility between the specified loop shape, the nominal plant phase, and robust closed-loop stability.

Remark 16.1 Note that, in contrast to the classical loop-shaping approach, the loop-shaping here is done without explicit regard for the nominal plant phase information. That is, closed-loop stability requirements are disregarded at this stage. Also, in contrast with conventional $\mathcal{H}_\infty$ design, the robust stabilization is done without frequency weighting. The design procedure described here is both simple and systematic and only assumes knowledge of elementary loop-shaping principles on the part of the designer. ◇

Remark 16.2 The preceding robust stabilization objective can also be interpreted as the more standard $\mathcal{H}_\infty$ problem formulation of minimizing the $\mathcal{H}_\infty$ norm of the frequency-weighted gain from disturbances on the plant input and output to the controller input and output as follows:

$$\begin{aligned}
\left\|\begin{bmatrix} I \\ K_\infty \end{bmatrix}(I+P_sK_\infty)^{-1}\tilde{M}_s^{-1}\right\|_\infty &= \left\|\begin{bmatrix} I \\ K_\infty \end{bmatrix}(I+P_sK_\infty)^{-1}\begin{bmatrix} I & P_s \end{bmatrix}\right\|_\infty \\
&= \left\|\begin{bmatrix} W_2 \\ W_1^{-1}K \end{bmatrix}(I+PK)^{-1}\begin{bmatrix} W_2^{-1} & PW_1 \end{bmatrix}\right\|_\infty \\
&= \left\|\begin{bmatrix} I \\ P_s \end{bmatrix}(I+K_\infty P_s)^{-1}\begin{bmatrix} I & K_\infty \end{bmatrix}\right\|_\infty \\
&= \left\|\begin{bmatrix} W_1^{-1} \\ W_2 P \end{bmatrix}(I+KP)^{-1}\begin{bmatrix} W_1 & KW_2^{-1} \end{bmatrix}\right\|_\infty
\end{aligned}$$

This shows how all the closed-loop objectives in equations (16.1) and (16.2) are incorporated. As an example, it is easy to see that the signal relationship in Figure 16.5 is given by

$$\begin{bmatrix} z_1 \\ z_2 \end{bmatrix} = \begin{bmatrix} W_2 \\ W_1^{-1}K \end{bmatrix}(I+PK)^{-1}\begin{bmatrix} W_2^{-1} & PW_1 \end{bmatrix}\begin{bmatrix} w_1 \\ w_2 \end{bmatrix}.$$

◇

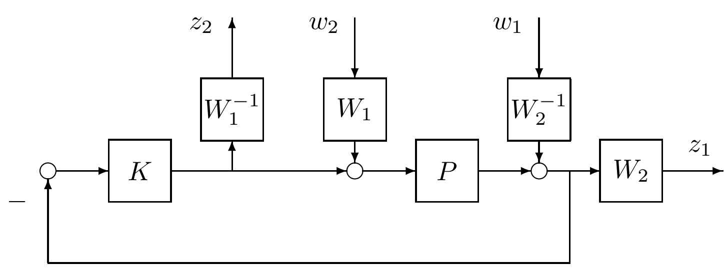

Figure 16.5: An equivalent $\mathcal{H}_\infty$ formulation

16.3 Justification for $\mathcal{H}_\infty$ Loop Shaping

The objective of this section is to provide justification for the use of parameter ϵ as a design indicator. We will show that ϵ is a measure of both closed-loop robust stability and the success of the design in meeting the loop-shaping specifications. Readers are encouraged to consult the original reference by McFarlane and Glover [1990] for further details.

We first examine the possibility of loop shape deterioration at frequencies of high loop gain (typically low-frequency). At low-frequency [in particular, $\omega \in (0, \omega_l)$], the deterioration in loop shape at plant output can be obtained by comparing $\underline{\sigma}(PW_1K_\infty W_2)$

to $\underline{\sigma}(P_s) = \underline{\sigma}(W_2PW_1)$. Note that

$$\underline{\sigma}(PK) = \underline{\sigma}(PW_1K_\infty W_2) = \underline{\sigma}(W_2^{-1}W_2PW_1K_\infty W_2) \geq \underline{\sigma}(W_2PW_1)\underline{\sigma}(K_\infty)/\kappa(W_2) \tag{16.3}$$

where $\kappa(\cdot)$ denotes condition number. Similarly, for loop shape deterioration at plant input, we have

$$\underline{\sigma}(KP) = \underline{\sigma}(W_1K_\infty W_2P) = \underline{\sigma}(W_1K_\infty W_2PW_1W_1^{-1}) \geq \underline{\sigma}(W_2PW_1)\underline{\sigma}(K_\infty)/\kappa(W_1). \tag{16.4}$$

In each case, $\underline{\sigma}(K_\infty)$ is required to obtain a bound on the deterioration in the loop shape at low-frequency. Note that the condition numbers $\kappa(W_1)$ and $\kappa(W_2)$ are selected by the designer.

Next, recalling that P_s denotes the shaped plant and that K_∞ robustly stabilizes the normalized coprime factorization of P_s with stability margin ϵ, we have

$$\left\| \begin{bmatrix} I \\ K_\infty \end{bmatrix} (I + P_sK_\infty)^{-1}\tilde{M}_s^{-1} \right\|_\infty \leq \epsilon^{-1} := \gamma \tag{16.5}$$

where $(\tilde{N}_s, \tilde{M}_s)$ is a normalized left coprime factorization of P_s, and the parameter γ is defined to simplify the notation to follow. The following result shows that $\underline{\sigma}(K_\infty)$ is explicitly bounded by functions of ϵ and $\underline{\sigma}(P_s)$, the minimum singular value of the shaped plant, and hence by equation (16.3) and (16.4) K_∞ will only have a limited effect on the specified loop shape at low-frequency.

Theorem 16.10 *Any controller K_∞ satisfying equation (16.5), where P_s is assumed square, also satisfies*

$$\underline{\sigma}(K_\infty(j\omega)) \geq \frac{\underline{\sigma}(P_s(j\omega)) - \sqrt{\gamma^2 - 1}}{\sqrt{\gamma^2 - 1}\,\underline{\sigma}(P_s(j\omega)) + 1}$$

for all ω such that

$$\underline{\sigma}(P_s(j\omega)) > \sqrt{\gamma^2 - 1}.$$

Furthermore, if $\underline{\sigma}(P_s) \gg \sqrt{\gamma^2 - 1}$, then $\underline{\sigma}(K_\infty(j\omega)) \gtrapprox 1/\sqrt{\gamma^2 - 1}$, where $\gtrapprox$ denotes asymptotically greater than or equal to as $\underline{\sigma}(P_s) \to \infty$.

Proof. First note that $\underline{\sigma}(P_s) > \sqrt{\gamma^2 - 1}$ implies that

$$I + P_sP_s^* > \gamma^2 I.$$

Further, since $(\tilde{N}_s, \tilde{M}_s)$ is a normalized left coprime factorization of P_s, we have

$$\tilde{M}_s\tilde{M}_s^* = I - \tilde{N}_s\tilde{N}_s^* = I - \tilde{M}_sP_sP_s^*\tilde{M}_s^*.$$

Then

$$\tilde{M}_s^*\tilde{M}_s = (I + P_sP_s^*)^{-1} < \gamma^{-2} I.$$

Now

$$\left\| \begin{bmatrix} I \\ K_\infty \end{bmatrix} (I + P_s K_\infty)^{-1} \tilde{M}_s^{-1} \right\|_\infty \leq \gamma$$

can be rewritten as

$$(I + K_\infty^* K_\infty) \leq \gamma^2 (I + K_\infty^* P_s^*)(\tilde{M}_s^* \tilde{M}_s)(I + P_s K_\infty). \tag{16.6}$$

We will next show that K_∞ is invertible. Suppose that there exists an x such that $K_\infty x = 0$, then $x^* \times$ equation (16.6) $\times\, x$ gives

$$\gamma^{-2} x^* x \leq x^* \tilde{M}_s^* \tilde{M}_s x,$$

which implies that $x = 0$ since $\tilde{M}_s^* \tilde{M}_s < \gamma^{-2} I$, and hence K_∞ is invertible. Equation (16.6) can now be written as

$$(K_\infty^{-*} K_\infty^{-1} + I) \leq \gamma^2 (K_\infty^{-*} + P_s^*) \tilde{M}_s^* \tilde{M}_s (K_\infty^{-1} + P_s). \tag{16.7}$$

Define W such that

$$(WW^*)^{-1} = I - \gamma^2 \tilde{M}_s^* \tilde{M}_s = I - \gamma^2 (I + P_s P_s^*)^{-1}.$$

Completing the square in equation (16.7) with respect to K_∞^{-1} yields

$$(K_\infty^{-*} + N^*)(WW^*)^{-1}(K_\infty^{-1} + N) \leq (\gamma^2 - 1) R^* R$$

where

$$\begin{aligned} N &= \gamma^2 P_s ((1 - \gamma^2) I + P_s^* P_s)^{-1} \\ R^* R &= (I + P_s^* P_s)((1 - \gamma^2) I + P_s^* P_s)^{-1}. \end{aligned}$$

Hence we have

$$R^{-*}(K_\infty^{-*} + N^*)(WW^*)^{-1}(K_\infty^{-1} + N) R^{-1} \leq (\gamma^2 - 1) I$$

and

$$\overline{\sigma}\left(W^{-1}(K_\infty^{-1} + N) R^{-1}\right) \leq \sqrt{\gamma^2 - 1}.$$

Use $\overline{\sigma}\left(W^{-1}(K_\infty^{-1} + N) R^{-1}\right) \geq \underline{\sigma}(W^{-1}) \overline{\sigma}(K_\infty^{-1} + N) \underline{\sigma}(R^{-1})$ to get

$$\overline{\sigma}(K_\infty^{-1} + N) \leq \sqrt{\gamma^2 - 1}\, \overline{\sigma}(W) \overline{\sigma}(R)$$

and use $\underline{\sigma}(K_\infty^{-1} + N) \geq \underline{\sigma}(K_\infty) - \overline{\sigma}(N)$ to get

$$\underline{\sigma}(K_\infty) \geq \left\{ (\gamma^2 - 1)^{1/2} \overline{\sigma}(W) \overline{\sigma}(R) + \overline{\sigma}(N) \right\}^{-1}. \tag{16.8}$$

Next, note that the eigenvalues of WW^*, N^*N, and R^*R can be computed as follows:

$$\lambda(WW^*) = \frac{1+\lambda(P_sP_s^*)}{1-\gamma^2+\lambda(P_sP_s^*)}$$

$$\lambda(N^*N) = \frac{\gamma^4\lambda(P_sP_s^*)}{(1-\gamma^2+\lambda(P_sP_s^*))^2}$$

$$\lambda(R^*R) = \frac{1+\lambda(P_sP_s^*)}{1-\gamma^2+\lambda(P_sP_s^*)}.$$

Therefore,

$$\overline{\sigma}(W) = \sqrt{\lambda_{\max}(WW^*)} = \left(\frac{1+\lambda_{\min}(P_sP_s^*)}{1-\gamma^2+\lambda_{\min}(P_sP_s^*)}\right)^{1/2} = \left(\frac{1+\underline{\sigma}^2(P_s)}{1-\gamma^2+\underline{\sigma}^2(P_s)}\right)^{1/2}$$

$$\overline{\sigma}(N) = \sqrt{\lambda_{\max}(N^*N)} = \frac{\gamma^2\sqrt{\lambda_{\min}(P_sP_s^*)}}{1-\gamma^2+\lambda_{\min}(P_sP_s^*)} = \frac{\gamma^2\underline{\sigma}(P_s)}{1-\gamma^2+\underline{\sigma}^2(P_s)}$$

$$\overline{\sigma}(R) = \sqrt{\lambda_{\max}(R^*R)} = \left(\frac{1+\lambda_{\min}(P_sP_s^*)}{1-\gamma^2+\lambda_{\min}(P_sP_s^*)}\right)^{1/2} = \left(\frac{1+\underline{\sigma}^2(P_s)}{1-\gamma^2+\underline{\sigma}^2(P_s)}\right)^{1/2}.$$

Substituting these formulas into equation (16.8), we have

$$\underline{\sigma}(K_\infty) \geq \left\{\frac{(\gamma^2-1)^{1/2}(1+\underline{\sigma}^2(P_s))+\gamma^2\underline{\sigma}(P_s)}{\underline{\sigma}^2(P_s)-(\gamma^2-1)}\right\}^{-1} = \frac{\underline{\sigma}(P_s))-\sqrt{\gamma^2-1}}{\sqrt{\gamma^2-1}\underline{\sigma}(P_s)+1}.$$

□

The main implication of Theorem 16.10 is that the bound on $\underline{\sigma}(K_\infty)$ depends only on the selected loop shape and the stability margin of the shaped plant. The value of $\gamma(=\epsilon^{-1})$ directly determines the frequency range over which this result is valid – a small γ (large ϵ) is desirable, as we would expect. Further, P_s has a sufficiently large loop gain; then so also will P_sK_∞ provided that $\gamma(=\epsilon^{-1})$ is sufficiently small.

In an analogous manner, we now examine the possibility of deterioration in the loop shape at high-frequency due to the inclusion of K_∞. Note that at high frequency [in particular, $\omega \in (\omega_h, \infty)$] the deterioration in plant output loop shape can be obtained by comparing $\overline{\sigma}(PW_1K_\infty W_2)$ to $\overline{\sigma}(P_s) = \overline{\sigma}(W_2PW_1)$. Note that, analogous to equation (16.3) and (16.4), we have

$$\overline{\sigma}(PK) = \overline{\sigma}(PW_1K_\infty W_2) \leq \overline{\sigma}(W_2PW_1)\overline{\sigma}(K_\infty)\kappa(W_2).$$

Similarly, the corresponding deterioration in plant input loop shape is obtained by comparing $\overline{\sigma}(W_1K_\infty W_2P)$ to $\overline{\sigma}(W_2PW_1)$, where

$$\overline{\sigma}(KP) = \overline{\sigma}(W_1K_\infty W_2P) \leq \overline{\sigma}(W_2PW_1)\overline{\sigma}(K_\infty)\kappa(W_1).$$

Hence, in each case, $\overline{\sigma}(K_\infty)$ is required to obtain a bound on the deterioration in the loop shape at high-frequency. In an identical manner to Theorem 16.10, we now show that $\overline{\sigma}(K_\infty)$ is explicitly bounded by functions of γ and $\overline{\sigma}(P_s)$, the maximum singular value of the shaped plant.

Theorem 16.11 *Any controller K_∞ satisfying equation (16.5) also satisfies*

$$\overline{\sigma}(K_\infty(j\omega)) \le \frac{\sqrt{\gamma^2-1}+\overline{\sigma}(P_s(j\omega))}{1-\sqrt{\gamma^2-1}\,\overline{\sigma}(P_s(j\omega))}$$

for all ω such that

$$\overline{\sigma}(P_s(j\omega)) < \frac{1}{\sqrt{\gamma^2-1}}.$$

Furthermore, if $\overline{\sigma}(P_s) \ll 1/\sqrt{\gamma^2-1}$, then $\overline{\sigma}(K_\infty(j\omega)) \lessapprox \sqrt{\gamma^2-1}$, where $\lessapprox$ denotes asymptotically less than or equal to as $\overline{\sigma}(P_s) \to 0$.

Proof. The proof of Theorem 16.11 is similar to that of Theorem 16.10 and is only sketched here: As in the proof of Theorem 16.10, we have $\tilde{M}_s^*\tilde{M}_s = (I+P_sP_s^*)^{-1}$ and

$$(I+K_\infty^*K_\infty) \le \gamma^2(I+K_\infty^*P_s^*)(\tilde{M}_s^*\tilde{M}_s)(I+P_sK_\infty). \tag{16.9}$$

Since $\overline{\sigma}(P_s) < \frac{1}{\sqrt{\gamma^2-1}}$,

$$I-\gamma^2P_s^*(I+P_sP_s^*)^{-1}P_s > 0$$

and there exists a spectral factorization

$$V^*V = I-\gamma^2P_s^*(I+P_sP_s^*)^{-1}P_s.$$

Now, completing the square in equation (16.9) with respect to K_∞ yields

$$(K_\infty^*+M^*)V^*V(K_\infty+M) \le (\gamma^2-1)Y^*Y$$

where

$$\begin{aligned} M &= \gamma^2P_s^*(I+(1-\gamma^2)P_sP_s^*)^{-1} \\ Y^*Y &= (\gamma^2-1)(I+P_sP_s^*)(I+(1-\gamma^2)P_sP_s^*)^{-1}. \end{aligned}$$

Hence we have

$$\overline{\sigma}\left(V(K_\infty+M)Y^{-1}\right) \le \sqrt{\gamma^2-1},$$

which implies

$$\overline{\sigma}(K_\infty) \le \frac{\sqrt{\gamma^2-1}}{\underline{\sigma}(V)\underline{\sigma}(Y^{-1})} + \overline{\sigma}(M). \tag{16.10}$$

As in the proof of Theorem 16.10, it is easy to show that

$$\underline{\sigma}(V) = \underline{\sigma}(Y^{-1}) = \left(\frac{1-(\gamma^2-1)\overline{\sigma}^2(P_s)}{1+\overline{\sigma}^2(P_s)}\right)^{1/2}$$

$$\overline{\sigma}(M) = \frac{\gamma^2\overline{\sigma}(P_s)}{1-(\gamma^2-1)\overline{\sigma}^2(P_s)}.$$

Substituting these formulas into equation (16.10), we have

$$\overline{\sigma}(K_\infty) \le \frac{(\gamma^2-1)^{1/2}(1+\overline{\sigma}^2(P_s))+\gamma^2\overline{\sigma}(P_s)}{1-(\gamma^2-1)\overline{\sigma}^2(P_s)} = \frac{\sqrt{\gamma^2-1}+\overline{\sigma}(P_s)}{1-\sqrt{\gamma^2-1}\,\overline{\sigma}(P_s)}.$$

□

The results in Theorems 16.10 and 16.11 confirm that γ (alternatively ϵ) indicates the compatibility between the specified loop shape and closed-loop stability requirements.

Theorem 16.12 *Let P be the nominal plant and let $K = W_1K_\infty W_2$ be the associated controller obtained from loop-shaping design procedure in the last section. Then if*

$$\left\|\begin{bmatrix} I \\ K_\infty \end{bmatrix}(I+P_sK_\infty)^{-1}\tilde{M}_s^{-1}\right\|_\infty \le \gamma$$

we have

$$\overline{\sigma}\left(K(I+PK)^{-1}\right) \le \gamma\overline{\sigma}(\tilde{M}_s)\overline{\sigma}(W_1)\overline{\sigma}(W_2) \tag{16.11}$$

$$\overline{\sigma}\left((I+PK)^{-1}\right) \le \min\left\{\gamma\overline{\sigma}(\tilde{M}_s)\kappa(W_2),\ 1+\gamma\overline{\sigma}(N_s)\kappa(W_2)\right\} \tag{16.12}$$

$$\overline{\sigma}\left(K(I+PK)^{-1}P\right) \le \min\left\{\gamma\overline{\sigma}(\tilde{N}_s)\kappa(W_1),\ 1+\gamma\overline{\sigma}(M_s)\kappa(W_1)\right\} \tag{16.13}$$

$$\overline{\sigma}\left((I+PK)^{-1}P\right) \le \frac{\gamma\overline{\sigma}(\tilde{N}_s)}{\underline{\sigma}(W_1)\underline{\sigma}(W_2)} \tag{16.14}$$

$$\overline{\sigma}\left((I+KP)^{-1}\right) \le \min\left\{1+\gamma\overline{\sigma}(\tilde{N}_s)\kappa(W_1),\ \gamma\overline{\sigma}(M_s)\kappa(W_1)\right\} \tag{16.15}$$

$$\overline{\sigma}\left(G(I+KP)^{-1}K\right) \le \min\left\{1+\gamma\overline{\sigma}(\tilde{M}_s)\kappa(W_2),\ \gamma\overline{\sigma}(N_s)\kappa(W_2)\right\} \tag{16.16}$$

where

$$\overline{\sigma}(\tilde{N}_s) = \overline{\sigma}(N_s) = \left(\frac{\overline{\sigma}^2(W_2PW_1)}{1+\overline{\sigma}^2(W_2PW_1)}\right)^{1/2} \tag{16.17}$$

$$\overline{\sigma}(\tilde{M}_s) = \overline{\sigma}(M_s) = \left(\frac{1}{1+\underline{\sigma}^2(W_2PW_1)}\right)^{1/2} \tag{16.18}$$

and $(\tilde{N}_s, \tilde{M}_s)$, (N_s, M_s) is a normalized left coprime factorization and right coprime factorization, respectively, of $P_s = W_2PW_1$.

Proof. Note that

$$\tilde{M}_s^* \tilde{M}_s = (I + P_s P_s^*)^{-1}$$

and

$$\tilde{M}_s \tilde{M}_s^* = I - \tilde{N}_s \tilde{N}_s^*.$$

Then

$$\overline{\sigma}^2(\tilde{M}_s) = \lambda_{\max}(\tilde{M}_s^* \tilde{M}_s) = \frac{1}{1 + \lambda_{\min}(P_s P_s^*)} = \frac{1}{1 + \underline{\sigma}^2(P_s)}$$

$$\overline{\sigma}^2(\tilde{N}_s) = 1 - \underline{\sigma}^2(\tilde{M}_s) = \frac{\overline{\sigma}^2(P_s)}{1 + \overline{\sigma}^2(P_s)}.$$

The proof for the normalized right coprime factorization is similar. All other inequalities follow from noting that

$$\left\| \begin{bmatrix} I \\ K_\infty \end{bmatrix} (I + P_s K_\infty)^{-1} \tilde{M}_s^{-1} \right\|_\infty \le \gamma$$

and

$$\begin{aligned} \left\| \begin{bmatrix} I \\ K_\infty \end{bmatrix} (I + P_s K_\infty)^{-1} \tilde{M}_s^{-1} \right\|_\infty &= \left\| \begin{bmatrix} W_2 \\ W_1^{-1} K \end{bmatrix} (I + PK)^{-1} \begin{bmatrix} W_2^{-1} & PW_1 \end{bmatrix} \right\|_\infty \\ &= \left\| \begin{bmatrix} W_1^{-1} \\ W_2 P \end{bmatrix} (I + KP)^{-1} \begin{bmatrix} W_1 & PW_2^{-1} \end{bmatrix} \right\|_\infty \end{aligned}$$

□

This theorem shows that all closed-loop objectives are guaranteed to have bounded magnitude and the bounds depend only on γ, W_1, W_2, and P.

16.4 Further Guidelines for Loop Shaping

Let $P = NM^{-1}$ be a normalized right coprime factorization. It was shown in Georgiou and Smith [1990] that

$$b_{\text{opt}}(P) \le \lambda(P) := \inf_{\text{Re}s>0} \underline{\sigma} \left(\begin{bmatrix} M(s) \\ N(s) \end{bmatrix} \right).$$

Hence a small $\lambda(P)$ would necessarily imply a small $b_{\text{opt}}(P)$. We shall now discuss the performance limitations implied by this relationship for a scalar system. The following argument is based on Vinnicombe [1993b], to which the reader is referred for further discussions. Let $z_1, z_2, \ldots, z_m$ and $p_1, p_2, \ldots, p_k$ be the open right-half plane zeros and poles of the plant P. Define

$$N_z(s) = \frac{z_1 - s}{z_1 + s} \frac{z_2 - s}{z_2 + s} \cdots \frac{z_m - s}{z_m + s}, \quad N_p(s) = \frac{p_1 - s}{p_1 + s} \frac{p_2 - s}{p_2 + s} \cdots \frac{p_k - s}{p_k + s}.$$

Then P can be written as

$$P(s) = P_0(s)N_z(s)/N_p(s)$$

where $P_0(s)$ has no open right-half plane poles or zeros. Let $N_0(s)$ and $M_0(s)$ be stable and minimum phase spectral factors:

$$N_0(s)N_0^\sim(s) = \left(1 + \frac{1}{P(s)P^\sim(s)}\right)^{-1}, \quad M_0(s)M_0^\sim(s) = (1 + P(s)P^\sim(s))^{-1}.$$

Then $P_0 = N_0/M_0$ is a normalized coprime factorization and (N_0N_z) and (M_0N_p) form a pair of normalized coprime factorizations of P. Thus

$$b_{\rm opt}(P) \le \sqrt{|N_0(s)N_z(s)|^2 + |M_0(s)N_p(s)|^2}, \quad \forall \mathrm{Re}(s) > 0. \tag{16.19}$$

Since N_0 and M_0 are both stable and have no zeros in the open right-half plane, $\ln(N_0(s))$ and $\ln(M_0(s))$ are both analytic in $\mathrm{Re}(s) > 0$ and so can be determined from their boundary values on $\mathrm{Re}(s) = 0$ via Poisson integrals (see also Problem 16.15):

$$\begin{aligned}
\ln|N_0(re^{j\theta})| &= \int_{-\infty}^{\infty} \ln\left(\frac{1}{\sqrt{1+1/|P(j\omega)|^2}}\right) K_\theta(\omega/r)\ d(\ln\omega) \\
\ln|M_0(re^{j\theta})| &= \int_{-\infty}^{\infty} \ln\left(\frac{1}{\sqrt{1+|P(j\omega)|^2}}\right) K_\theta(\omega/r)\ d(\ln\omega)
\end{aligned}$$

where $r > 0$, $-\pi/2 < \theta < \pi/2$, and

$$K_\theta(\omega/r) = \frac{1}{\pi}\frac{2(\omega/r)[1+(\omega/r)^2]\cos\theta}{[1-(\omega/r)^2]^2 + 4(\omega/r)^2\cos^2\theta}$$

The function $K_\theta(\omega/r)$ is plotted in Figure 16.6 against logarithmic frequency for various values of θ. Note that the function is symmetric to $\omega = r$ in $\log\omega$ and it attends the maximum at $\omega = r$. The function converges to an impulse function at $\omega = r$ when θ approaches $90^{\rm o}$; that is, when $|N_0(s)|$ or $|M_0(s)|$ is evaluated close to the imaginary axis.

Since the kernel function $K_\theta(\omega/r)$ has the greatest weighting near $\omega = r$, the Poisson integral is largely determined by the frequency response near that frequency. Thus it is clear that $|N_0(re^{j\theta})|$ will be small if $|P(j\omega)|$ is small near $\omega = r$. Similarly, $|M_0(re^{j\theta})|$ will be small if $|P(j\omega)|$ is large near $\omega = r$.

It is also important to note that a very large percentage of weighting is concentrated in a very narrow frequency range for a large θ (i.e., when $s = re^{j\theta}$ has a much larger imaginary part than the real part). Hence $|N_0(re^{j\theta})|$ and $|M_0(re^{j\theta})|$ will essentially be determined by $|P(j\omega)|$ in a very narrow frequency range near $\omega = r$ when θ is large. On the other hand, when θ is small, a larger range of frequency response $|P(j\omega)|$ around $\omega = r$ will have affect on the value $|N_0(re^{j\theta})|$ and $|M_0(re^{j\theta})|$. (This, in fact, will imply

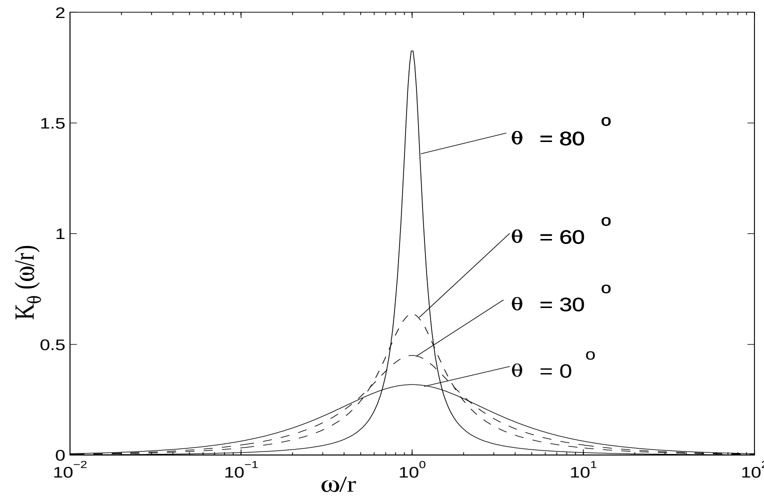

Figure 16.6: $K_\theta(\omega/r)$ vs. normalized frequency ω/r

that a right-plane zero (pole) with a much larger real part than the imaginary part will have much worse effect on the performance than a right-plane zero (pole) with a much larger imaginary part than the real part.)

Let $s = re^{j\theta}$. Consider again the bound of equation (16.19) and note that $N_z(z_i) = 0$ and $N_p(p_j) = 0$, we see that there are several ways in which the bound may be small (i.e., $b_{\text{opt}}(P)$ is small).

▷ $|N_z(s)|$ and $|N_p(s)|$ are both small for some s. That is, $|N_z(s)| \approx 0$ (i.e., s is close to a right-half plane zero of P) and $|N_p(s)| \approx 0$ (i.e., s is close to a right-half plane pole of P). This is only possible if $P(s)$ has a right-half plane zero near a right-half plane pole. (See Example 16.1.)

▷ $|N_z(s)|$ and $|M_0(s)|$ are both small for some s. That is, $|N_z(s)| \approx 0$ (i.e., s is close to a right-half plane zero of P) and $|M_0(s)| \approx 0$ (i.e., $|P(j\omega)|$ is large around $\omega = |s| = r$). This is only possible if $|P(j\omega)|$ is large around $\omega = r$, where r is the modulus of a right-half plane zero of P. (See Example 16.2.)

▷ $|N_p(s)|$ and $|N_0(s)|$ are both small for some s. That is, $|N_p(s)| \approx 0$ (i.e., s is close to a right-half plane pole of P) and $|N_0(s)| \approx 0$ (i.e., $|P(j\omega)|$ is small around $\omega = |s| = r$). This is only possible if $|P(j\omega)|$ is small around $\omega = r$, where r is the modulus of a right-half plane pole of P. (See Example 16.3.)

▷ $|N_0(s)|$ and $|M_0(s)|$ are both small for some s. That is, $|N_0(s)| \approx 0$ (i.e., $|P(j\omega)|$ is small around $\omega = |s| = r$) and $|M_0(s)| \approx 0$ (i.e., $|P(j\omega)|$ is large around $\omega = |s| = r$). The only way in which $|P(j\omega)|$ can be both small and large at frequencies near $\omega = r$ is that $|P(j\omega)|$ is approximately equal to 1 and the absolute value of the slope of $|P(j\omega)|$ is large. (See Example 16.4.)

Example 16.1 Consider an unstable and nonminimum phase system

$$P_1(s) = \frac{K(s-r)}{(s+1)(s-1)}.$$

The frequency responses of $P_1(s)$ with $r = 0.9$ and $K = 0.1, 1,$ and 10 are shown in Figure 16.7. The following table shows that $b_{\text{opt}}(P_1)$ will be very small for all K whenever r is close to 1 (i.e., whenever there is an unstable pole close to an unstable zero).

$K = 0.1$	r	0.5	0.7	0.9	1.1	1.3	1.5
	$b_{\text{opt}}(P_1)$	0.0125	0.0075	0.0025	0.0025	0.0074	0.0124
$K = 1$	r	0.5	0.7	0.9	1.1	1.3	1.5
	$b_{\text{opt}}(P_1)$	0.1036	0.0579	0.0179	0.0165	0.0457	0.0706
$K = 10$	r	0.5	0.7	0.9	1.1	1.3	1.5
	$b_{\text{opt}}(P_1)$	0.0658	0.0312	0.0088	0.0077	0.0208	0.0318

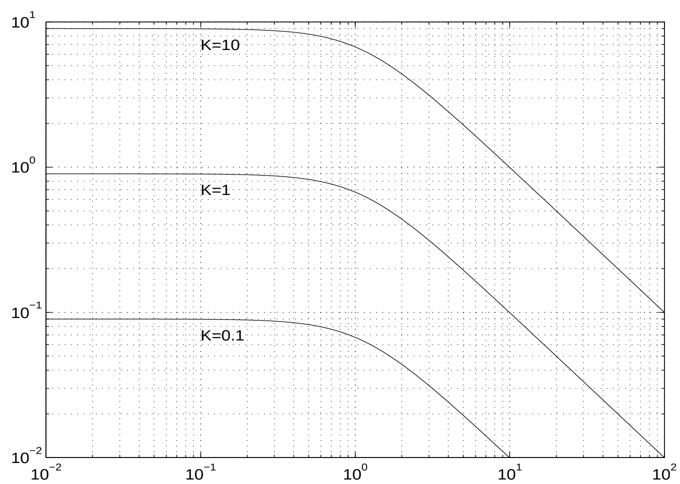

Figure 16.7: Frequency responses of P_1 for $r = 0.9$ and $K = 0.1, 1,$ and 10

Example 16.2 Consider a nonminimum phase plant

$$P_2(s) = \frac{K(s-1)}{s(s+1)}.$$

The frequency responses of $P_2(s)$ with $K = 0.1, 1$, and 10 are shown in Figure 16.8. The following table shows clearly that $b_{\mathrm{opt}}(P_2)$ will be small if $|P_2(j\omega)|$ is large around $\omega = 1$, the modulus of the right-half plane zero.

K	0.01	0.1	1	10	100
$b_{\mathrm{opt}}(P_2)$	0.7001	0.6451	0.3827	0.0841	0.0098

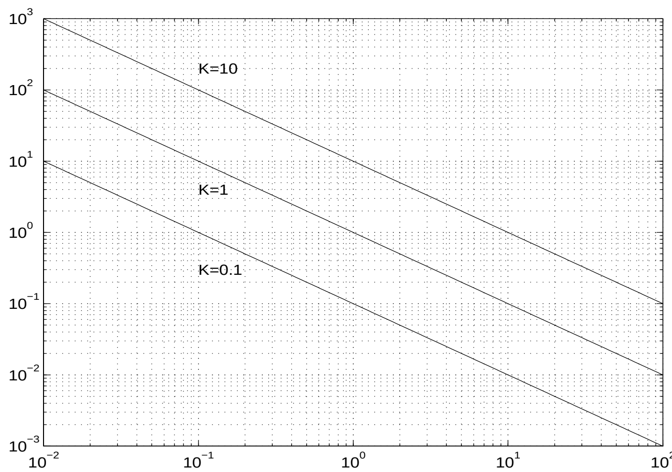

Figure 16.8: Frequency responses of P_2 for $K = 0.1, 1$, and 10

Note that $b_{\mathrm{opt}}(L/s) = 0.707$ for any L and $b_{\mathrm{opt}}(P_2) \longrightarrow 0.707$ as $K \longrightarrow 0$. This is because $|P_2(j\omega)|$ around the frequency of the right-half plane zero is very small as $K \longrightarrow 0$.

Next consider a plant with a pair of complex right-half plane zeros:

$$P_3(s) = \frac{K[(s-\cos\theta)^2 + \sin^2\theta]}{s[(s+\cos\theta)^2 + \sin^2\theta]}.$$

The magnitude frequency response of P_3 is the same as that of P_2 for the same K. The optimal $b_{\mathrm{opt}}(P_3)$ for various θ's are listed in the following table:

$K = 0.1$	θ (degree)	0	45	60	80	85
	$b_{\text{opt}}(P_3)$	0.5952	0.6230	0.6447	0.6835	0.6950
$K = 1$	θ (degree)	0	45	60	80	85
	$b_{\text{opt}}(P_3)$	0.2588	0.3078	0.3568	0.4881	0.5512
$K = 10$	θ (degree)	0	45	60	80	85
	$b_{\text{opt}}(P_3)$	0.0391	0.0488	0.0584	0.0813	0.0897

It can also be concluded from the table that $b_{\text{opt}}(P_3)$ will be small if $|P_3(j\omega)|$ is large around the frequency of $\omega = 1$ (the modulus of the right-half plane zero). It can be further concluded that, for zeros with the same modulus, $b_{\text{opt}}(P_3)$ will be smaller for a plant with relatively larger real part zeros than for a plant with relatively larger imaginary part zeros (i.e., a pair of real right-half plane zeros has a much worse effect on the performance than a pair of almost pure imaginary axis right-half plane zeros of the same modulus).

Example 16.3 Consider an unstable plant

$$P_4(s) = \frac{K(s+1)}{s(s-1)}.$$

The magnitude frequency response of P_4 is again the same as that of P_2 for the same K. The following table shows that $b_{\text{opt}}(P_4)$ will be small if $|P_4(j\omega)|$ is small around $\omega = 1$ (the modulus of the right-half plane pole).

K	0.01	0.1	1	10	100
$b_{\text{opt}}(P_4)$	0.0098	0.0841	0.3827	0.6451	0.7001

Note that $b_{\text{opt}}(P_4) \longrightarrow 0.707$ as $K \longrightarrow \infty$. This is because $|P_4(j\omega)|$ is very large around the frequency of the modulus of the right-half plane pole as $K \longrightarrow \infty$.

Next consider a plant with complex right-half plane poles:

$$P_5(s) = \frac{K[(s+\cos\theta)^2 + \sin^2\theta]}{s[(s-\cos\theta)^2 + \sin^2\theta]}.$$

The optimal $b_{\text{opt}}(P_5)$ for various θ's are listed in the following table:

	θ (degree)	0	45	60	80	85
$K = 0.1$	$b_{\text{opt}}(P_5)$	0.0391	0.0488	0.0584	0.0813	0.0897
	θ (degree)	0	45	60	80	85
$K = 1$	$b_{\text{opt}}(P_5)$	0.2588	0.3078	0.3568	0.4881	0.5512
	θ (degree)	0	45	60	80	85
$K = 10$	$b_{\text{opt}}(P_5)$	0.5952	0.6230	0.6447	0.6835	0.6950

It can also be concluded from the table that $b_{\text{opt}}(P_5)$ will be small if $|P_5(j\omega)|$ is small around the frequency of the modulus of the right-half plane pole. It can be further concluded that, for poles with the same modulus, $b_{\text{opt}}(P_5)$ will be smaller for a plant with relatively larger real part poles than for a plant with relatively larger imaginary part poles (i.e., a pair of real right-half plane poles has a much worse effect on the performance than a pair of almost pure imaginary axis right-half plane poles of the same modulus).

Example 16.4 Let a stable and minimum phase transfer function be

$$P_6(s) = \frac{K(0.2s+1)^4}{s(s+1)^4}.$$

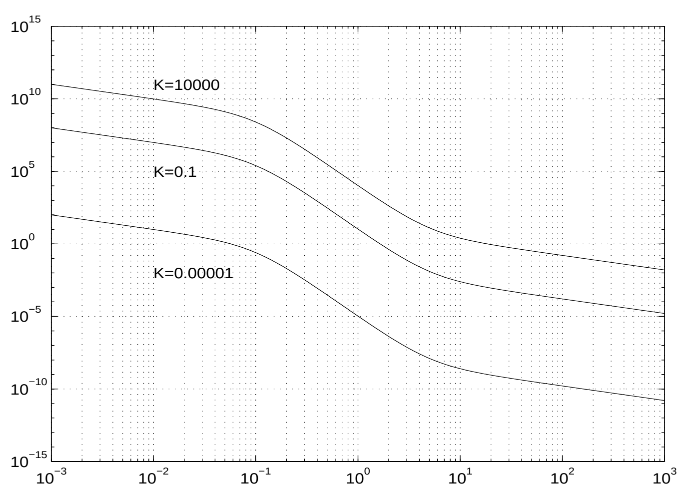

Figure 16.9: Frequency response of P_6 for $K = 10^{-5}, 10^{-1}$ and 10^4

The frequency responses of P_6 with $K = 10^{-5}, 10^{-1}$, and 10^4 are shown in Figure 16.9. It is clear that the slope of the frequency response near the crossover frequency for $K = 10^{-5}$ is not too large, which implies a reasonably good loop shape. Thus we should expect $b_{\rm opt}(P_6)$ to be not too small. A similar conclusion applies to $K = 10^4$. On the other hand, the slope of the frequency response near the crossover frequency for $K = 0.1$ is quite large which implies a bad loop shape. Thus we should expect $b_{\rm opt}(P_6)$ to be quite small. This is clear from the following table:

K	10^{-5}	10^{-3}	0.1	1	10	10^2	10^4
$b_{\rm opt}(P_6)$	0.3566	0.0938	0.0569	0.0597	0.0765	0.1226	0.4933

Based on the preceding discussion, we can give some guidelines for the loop-shaping design.

♡ The loop transfer function should be shaped in such a way that it has low gain around the frequency of the modulus of any right-half plane zero z. Typically, it requires that the crossover frequency be much smaller than the modulus of the right-half plane zero; say, $\omega_c < |z|/2$ for any real zero and $\omega_c < |z|$ for any complex zero with a much larger imaginary part than the real part (see Figure 16.6).

♡ The loop transfer function should have a large gain around the frequency of the modulus of any right-half plane pole.

♡ The loop transfer function should not have a large slope near the crossover frequencies.

These guidelines are consistent with the rules used in classical control theory (see Bode [1945] and Horowitz [1963]).

16.5 Notes and References

The $\mathcal{H}_\infty$ loop-shaping using normalized coprime factorization was developed by McFarlane and Glover [1990, 1992], on which most parts of this chapter is based. In the same references, some design examples were also shown. The method has been applied to the design of scheduled controllers for a VSTOL aircraft in Hyde and Glover [1993]. Some limitations of this loop-shaping design are discussed in detail in Vinnicombe [1993b] (on which Section 16.4 is based) and Christian and Freudenberg [1994]. The robust stabilization of normalized coprime factors is closely related to the robustness in the gap metric and ν-gap metric, which will be discussed in the next chapter, see El-Sakkary [1985], Georgiou and Smith [1990], Glover and McFarlane [1989], McFarlane, Glover, and Vidyasagar [1990], Qiu and Davison [1992a, 1992b], Vinnicombe [1993a, 1993b], Vidyasagar [1984, 1985], Zhu [1989], and references therein.

16.6 Problems

Problem 16.1 Consider a feedback system with $G(s) = \dfrac{1}{s-2}$. Compute by hand $\epsilon_{\max}$, the maximum stability radius for a normalized coprime factor perturbation of $G(s)$.

Problem 16.2 In Corollary 16.2, find the parameterization of all $\mathcal{H}_\infty$ controllers.

Problem 16.3 Let $P_\Delta = (N + \Delta_N)(M + \Delta_M)^{-1}$ be a right coprime factor perturbed plant with a nominal plant $P = NM^{-1}$, where (N, M) is a pair of normalized right coprime factorization. Formulate the corresponding robust stabilization problem as an $\mathcal{H}_\infty$ control problem and find a stabilizing controller using the $\mathcal{H}_\infty$ formulas in Chapter 14. Are there any connections between this stabilizing controller and the controller obtained in this chapter for left coprime stabilization?

Problem 16.4 Let P have coprime factorizations $P = NM^{-1} = \tilde{M}^{-1}\tilde{N}$. Then there exist $U, V, \tilde{U}, \tilde{V} \in \mathcal{H}_\infty$ such that

$$\begin{bmatrix} M & U \\ N & V \end{bmatrix} \begin{bmatrix} \tilde{V} & -\tilde{U} \\ \tilde{N} & \tilde{M} \end{bmatrix} = I.$$

Furthermore, all stabilizing controllers for P can be written as

$$K = (U + MQ)(V + NQ)^{-1}, \quad Q \in \mathcal{H}_\infty.$$

Show that

$$\begin{bmatrix} K \\ I \end{bmatrix} (I + PK)^{-1}\tilde{M}^{-1} = \begin{bmatrix} U + MQ \\ V + NQ \end{bmatrix}.$$

Suppose $P = NM^{-1} = \tilde{M}^{-1}\tilde{N}$ are normalized coprime factorizations. Show that

$$b_{P,K}^{-1} = \left\| \begin{bmatrix} U \\ V \end{bmatrix} + \begin{bmatrix} M \\ N \end{bmatrix} Q \right\|_\infty = \left\| \begin{bmatrix} R + Q \\ I \end{bmatrix} \right\|_\infty$$

where $R = M^\sim U + N^\sim V$.

Problem 16.5 Let K be a controller that stabilizes the plant P. Show that

1. K stabilizes $\tilde{P} = P + \Delta_a$ such that $\Delta_a \in \mathcal{H}_\infty$ and $\|\Delta_a\| < b_{P,K}$;
2. K stabilizes $\tilde{P} = P(I + \Delta_m)$ such that $\Delta_m \in \mathcal{H}_\infty$ and $\|\Delta_m\| < b_{P,K}$;
3. K stabilizes $\tilde{P} = (I + \Delta_m)P$ such that $\Delta_m \in \mathcal{H}_\infty$ and $\|\Delta_m\| < b_{P,K}$;
4. K stabilizes $\tilde{P} = P(I + \Delta_f)^{-1}$ such that $\Delta_f \in \mathcal{H}_\infty$ and $\|\Delta_f\| < b_{P,K}$;
5. K stabilizes $\tilde{P} = (I + \Delta_f)^{-1}P$ such that $\Delta_f \in \mathcal{H}_\infty$ and $\|\Delta_f\| < b_{P,K}$.

Discuss the possible implications of the preceding results.

Problem 16.6 Let K be a controller that stabilizes the plant P. Show that

1. any controller in the form of $\tilde{K} = (U + \Delta_U)(V + \Delta_V)^{-1}$ such that $\Delta_U, \Delta_V \in \mathcal{H}_\infty$ and $\left\| \begin{bmatrix} \Delta_U \\ \Delta_V \end{bmatrix} \right\|_\infty < b_{P,K}$ also stabilizes P;
2. any controller $\tilde{K} = K + \Delta_a$ such that $\Delta_a \in \mathcal{H}_\infty$ and $\|\Delta_a\| < b_{P,K}$ also stabilizes P;
3. any controller $\tilde{K} = K(I + \Delta_m)$ such that $\Delta_m \in \mathcal{H}_\infty$ and $\|\Delta_m\| < b_{P,K}$ also stabilizes P;
4. any controller $\tilde{K} = (I + \Delta_m)K$ such that $\Delta_m \in \mathcal{H}_\infty$ and $\|\Delta_m\| < b_{P,K}$ also stabilizes P;
5. any controller $\tilde{K} = K(I + \Delta_f)^{-1}$ such that $\Delta_f \in \mathcal{H}_\infty$ and $\|\Delta_f\| < b_{P,K}$ also stabilizes P;
6. any controller $\tilde{K} = (I + \Delta_f)^{-1}K$ such that $\Delta_f \in \mathcal{H}_\infty$ and $\|\Delta_f\| < b_{P,K}$ also stabilizes P.

Discuss the possible implications of the preceding results.

Problem 16.7 Let an uncertain plant be given by

$$P_\delta = \frac{s + \alpha}{s^2 + 2\zeta s + 1}, \quad \alpha \in [1, 3], \quad \zeta \in [0.2, 0.4]$$

and let a nominal model be

$$P = \frac{s + \alpha_0}{s^2 + 2\zeta_0 s + 1}.$$

1. Let $\alpha_0 = 2$ and $\zeta_0 = 0.3$. Find the largest possible $\|\Delta_{\text{add}}\|_\infty$ and $\|\Delta_{\text{mul}}\|_\infty$ where
$$\Delta_{\text{add}} = P_\delta - P, \quad \Delta_{\text{mul}} = (P_\delta - P)/P.$$
2. Let $\alpha_0 = 2$ and $\zeta_0 = 0.3$. Show that $P = N/M$ with
$$N = \frac{s + 2}{s^2 + 1.9576s + 2.2361}, \quad M = \frac{s^2 + 0.6s + 1}{s^2 + 1.9576s + 2.2361}$$
is a normalized coprime factorization. Now let
$$N_\delta = \frac{s + \alpha}{s^2 + 1.9576s + 2.2361}, \quad M_\delta = \frac{s^2 + 2\zeta s + 1}{s^2 + 1.9576s + 2.2361}$$
$$\Delta_n = N_\delta - N, \quad \Delta_m = M_\delta - M.$$
Find the largest possible $\left\| \begin{bmatrix} \Delta_n & \Delta_m \end{bmatrix} \right\|_\infty$.

3. In part 2, let (N_δ, M_δ) be a normalized coprime factorization of P_δ. Find the largest possible $\left\| \begin{bmatrix} \Delta_n & \Delta_m \end{bmatrix} \right\|_\infty$.
4. Find the optimal nominal α_0 and ζ_0 such that the largest possible $\|\Delta_{\mathrm{add}}\|_\infty$, $\|\Delta_{\mathrm{mul}}\|_\infty$, and $\left\| \begin{bmatrix} \Delta_n & \Delta_m \end{bmatrix} \right\|_\infty$ are minimized, respectively.

Discuss the advantages of each uncertainty modeling method in terms of robust stabilizations.

Problem 16.8 Let $P = \dfrac{-10}{s(s-1)}$. Design (a) a precompensator W of order no greater than 2 such that the crossover frequency $\omega_c \le 2$ and $b_{\mathrm{opt}}(WP)$ is as large as possible; (b) find the optimal loop-shaping controller $K = K_\infty W$ with the W obtained in part (a).

Problem 16.9 Let $P = \dfrac{100(1-s)}{s(s+10)}$. Design (a) a precompensator W of order no greater than 2 such that the crossover frequency $\omega_c \ge 1$ and $b_{\mathrm{opt}}(WP)$ is as large as possible; (b) find the optimal loop-shaping controller $K = K_\infty W$ with the W obtained in part (a).

Problem 16.10 Let $G(s) = \left[\begin{array}{c|c} A & B \\ \hline C & 0 \end{array}\right]$ and $G(s) = NM^{-1}$ with

$$\begin{bmatrix} N \\ M \end{bmatrix} = \left[\begin{array}{c|c} A+BF & B \\ \hline C & 0 \\ F & I \end{array}\right]$$

where F is chosen such that NM^{-1} is a normalized right coprime factorization. Let $\begin{bmatrix} \hat{N} \\ \hat{M} \end{bmatrix}$ be an rth order balanced truncation of $\begin{bmatrix} N \\ M \end{bmatrix}$. Show that $\begin{bmatrix} \hat{N} \\ \hat{M} \end{bmatrix}$ is also a normalized right coprime factorization.

Problem 16.11 (Reduced-Order Controllers by Controller Model Reduction; see McFarlane and Glover [1990], Zhou and Chen [1995].) Let $G(s) = \left[\begin{array}{c|c} A & B \\ \hline C & 0 \end{array}\right] = \tilde{M}^{-1}\tilde{N}$ be a normalized left coprime factorization and let $K(s)$ be a suboptimal controller given in Corollary 18.2 (with performance γ). Let $K = UV^{-1}$ be a right coprime factorization

$$\begin{bmatrix} U \\ V \end{bmatrix} = \left[\begin{array}{c|c} A - BB^*X_\infty & -YC^* \\ \hline -C & I \\ -B^*X_\infty & 0 \end{array}\right]$$

and $\hat{U}, \hat{V} \in \mathcal{RH}_\infty$ be approximations of U and V. Define

$$\epsilon := \left\| \begin{bmatrix} U \\ V \end{bmatrix} - \begin{bmatrix} \hat{U} \\ \hat{V} \end{bmatrix} \right\|_\infty$$

and $K_r = \hat{U}\hat{V}^{-1}$. Show that K_r is a stabilizing controller for G if $\epsilon < 1$ and

$$\left\| \begin{bmatrix} K_r \\ I \end{bmatrix} (I + GK_r)^{-1} \tilde{M}^{-1} \right\|_\infty = \left\| \begin{bmatrix} K_r \\ I \end{bmatrix} (I + GK_r)^{-1} \begin{bmatrix} I & G \end{bmatrix} \right\|_\infty < \frac{\gamma}{1-\epsilon}.$$

Problem 16.12 (Reduced Order Controllers by Plant Model Reduction; see McFarlane and Glover [1990].) Let $G = \tilde{M}^{-1}\tilde{N}$ be a normalized left coprime factorization and let K be a stabilizing controller such that

$$\left\| \begin{bmatrix} K \\ I \end{bmatrix} (I + GK)^{-1} \tilde{M}^{-1} \right\|_\infty \le \delta^{-1}.$$

Let $G_r := \tilde{M}_r^{-1}\tilde{N}_r$ be an approximation of G and

$$\epsilon := \left\| \begin{bmatrix} \tilde{M} - \tilde{M}_r & \tilde{N} - \tilde{N}_r \end{bmatrix} \right\|_\infty < \delta.$$

(a) Show that K stabilizes G_r and

$$\left\| \begin{bmatrix} K \\ I \end{bmatrix} (I + G_r K)^{-1} \tilde{M}_r^{-1} \right\|_\infty \le (\delta - \epsilon)^{-1}.$$

(b) Let $W(s), W^{-1}(s) \in \mathcal{RH}_\infty$ be obtained from the following spectral factorization:

$$W^{-1}W^{-*} = \tilde{M}_r\tilde{M}_r^* + \tilde{N}_r\tilde{N}_r^*.$$

Show that $\|W\|_\infty \le \dfrac{1}{1-\epsilon}$ and $\left\|W^{-1}\right\|_\infty \le 1 + \epsilon$.

(c) Show that

$$\delta_{rn}^{-1} := \inf_{K_1} \left\| \begin{bmatrix} K_1 \\ I \end{bmatrix} (I + G_r K_1)^{-1} (W\tilde{M}_r)^{-1} \right\|_\infty$$

$$= \inf_{K_1} \left\| \begin{bmatrix} K_1 \\ I \end{bmatrix} (I + G_r K_1)^{-1} \begin{bmatrix} I & G_r \end{bmatrix} \right\|_\infty \le \frac{\left\|W^{-1}\right\|_\infty}{\delta - \epsilon} \le \frac{1+\epsilon}{\delta - \epsilon}.$$

and

$$\left\| \begin{bmatrix} K_1 \\ I \end{bmatrix} (I + G_r K_1)^{-1} \tilde{M}_r^{-1} \right\|_\infty \le \delta_{rn}^{-1} \|W\|_\infty .$$

(d) With the controller K_1 given in (c), show that

$$\left\| \begin{bmatrix} K_1 \\ I \end{bmatrix} (I+GK_1)^{-1}\tilde{M}^{-1} \right\|_\infty = \left\| \begin{bmatrix} K_1 \\ I \end{bmatrix} (I+GK_1)^{-1} \begin{bmatrix} I & G \end{bmatrix} \right\|_\infty \le \delta_{\text{red}}^{-1}$$

where

$$\delta_{\text{red}} := \frac{\delta_{rn}}{\|W\|_\infty} - \epsilon \le \frac{\delta - \epsilon}{\|W^{-1}\|_\infty \|W\|_\infty} - \epsilon \le \frac{1-\epsilon}{1+\epsilon}(\delta - \epsilon) - \epsilon.$$

Note that if $\tilde{N}_r$ and $\tilde{M}_r$ are the kth-order balanced truncation of $\tilde{N}$ and $\tilde{M}$, then $\delta = \delta_{rn} = \sqrt{1-\sigma_1^2}$, $\delta_{\text{red}} = \delta - \epsilon$, and $\epsilon \le 2\sum_{i=k+1}^n \sigma_i$, where σ_i are the Hankel singular values of $\begin{bmatrix} \tilde{M} & \tilde{N} \end{bmatrix}$.

(e) Show that

$$\tilde{\delta}_r^{-1} := \inf_{K_2} \left\| \begin{bmatrix} K_2 \\ I \end{bmatrix} (I+G_rK_2)^{-1}\tilde{M}_r^{-1} \right\|_\infty \le (\delta - \epsilon)^{-1}.$$

(f) With the controller K_2 given in (e), show that

$$\left\| \begin{bmatrix} K_2 \\ I \end{bmatrix} (I+GK_2)^{-1}\tilde{M}^{-1} \right\|_\infty = \left\| \begin{bmatrix} K_2 \\ I \end{bmatrix} (I+GK_2)^{-1} \begin{bmatrix} I & G \end{bmatrix} \right\|_\infty$$

$$\le (\tilde{\delta}_r - \epsilon)^{-1} \le (\delta - 2\epsilon)^{-1}.$$

Again note that if $\tilde{N}_r$ and $\tilde{M}_r$ are the kth-order balanced truncation of $\tilde{N}$ and $\tilde{M}$, then $\tilde{\delta}_r = \delta$.

(Note that K_1 and K_2 are reduced-order controllers.)

Problem 16.13 Let $G(s) = \left[\begin{array}{c|c} A & B \\ \hline C & 0 \end{array}\right] = \tilde{M}^{-1}\tilde{N}$ be a normalized left coprime factorization and let $K(s)$ be a suboptimal controller given in Corollary 18.2 (with performance γ):

$$K(s) = \left[\begin{array}{c|c} A - BB^*X_\infty - YC^*C & -YC^* \\ \hline -B^*X_\infty & 0 \end{array}\right]$$

where

$$X_\infty = \frac{\gamma^2}{\gamma^2-1} Q \left(I - \frac{\gamma^2}{\gamma^2-1} YQ \right)^{-1}$$

and

$$AY + YA^* - YC^*CY + BB^* = 0$$

$$Q(A - YC^*C) + (A - YC^*C)^*Q + C^*C = 0.$$

Suppose Y and Q are balanced; that is,

$$Y = Q = \operatorname{diag}(\sigma_1, \ldots, \sigma_r, \sigma_{r+1}, \ldots, \sigma_n) = \operatorname{diag}(\Sigma_1, \Sigma_2)$$

and let $G(s)$ be partitioned accordingly as

$$G(s) = \left[\begin{array}{cc|c} A_{11} & A_{12} & B_1 \\ A_{21} & A_{22} & B_2 \\ \hline C_1 & C_2 & 0 \end{array}\right].$$

Denote $Y_1 = \Sigma_1$ and $X_1 = \frac{\gamma^2}{\gamma^2-1}\Sigma_1\left(I - \frac{\gamma^2}{\gamma^2-1}\Sigma_1^2\right)^{-1}$. Show that

$$K_r(s) = \left[\begin{array}{c|c} A_{11} - B_1B_1^*X_1 - Y_1C_1^*C_1 & -Y_1C_1^* \\ \hline -B_1^*X_1 & 0 \end{array}\right]$$

is exactly the reduced-order controller obtained from the last problem with balanced model reduction procedure. (It is also interesting to note that

$$Q = X(I + YX)^{-1}$$

where $X = X^* \geq 0$ is the stabilizing solution to

$$XA + A^*X - XBB^*X + C^*C = 0.$$

Hence balancing Y and Q is equivalent to balancing X and Y. This is called Riccati balancing; see Jonckheere and Silverman [1983].)

Problem 16.14 Apply the controller reduction methods in the last three problems, respectively, to a satellite system $G(s) = \left[\begin{array}{c|c} A & B \\ \hline C & 0 \end{array}\right]$ where

$$A = \begin{bmatrix} 0 & 1 & 0 & 0 \\ 0 & 0 & 0 & 0 \\ 0 & 0 & 0 & 1 \\ 0 & 0 & -1.539^2 & -2 \times 0.003 \times 1.539 \end{bmatrix}, \quad B = \begin{bmatrix} 0 \\ 1.7319 \times 10^{-5} \\ 0 \\ 3.7859 \times 10^{-4} \end{bmatrix},$$

$$C = \begin{bmatrix} 1 & 0 & 1 & 0 \end{bmatrix}, \quad D = 0.$$

Compare the results (see McFarlane and Glover [1990] for further details).

Problem 16.15 Let $f(s)$ be analytic in the closed right-half plane and suppose

$$\lim_{r\to\infty} \max_{\theta\in[-\pi/2,\pi/2]} \frac{|f(re^{j\theta})}{r} = 0.$$

Then the Poisson integral formula (see, for example, Freudenberg and Looze [1988], page 37) says that $f(s)$ at any point $s = x + jy$ in the open right-half plane can be recovered from $f(j\omega)$ via the integral relation:

$$f(s) = \frac{1}{\pi}\int_{-\infty}^{\infty} f(j\omega)\frac{x}{x^2+(y-\omega)^2}d\omega.$$

Let $s = re^{j\theta}$ (i.e., $x = r\cos\theta$ and $y = r\sin\theta$) with $r > 0$ and $-\pi/2 < \theta < \pi/2$. Suppose $f(j\omega) = f(-j\omega)$. Show that

$$f(re^{j\theta}) = \int_{-\infty}^{\infty} f(j\omega)K_\theta(\omega/r)\ d(\ln\omega)$$

where

$$K_\theta(\omega/r) = \frac{1}{\pi}\frac{2(\omega/r)[1+(\omega/r)^2]\cos\theta}{[1-(\omega/r)^2]^2+4(\omega/r)^2\cos^2\theta}$$